High resolution partial fingerprint alignment using pore–valley descriptors

Qijun Zhao, David Zhang*, Lei Zhang, Nan Luo

Biometrics Research Centre, Department of Computing, The Hong Kong Polytechnic University, Hung Hom, Kowloon, Hong Kong

ARTICLE INFO

ABSTRACT

This paper discusses the alignment of high resolution partial fingerprints, which is a crucial step in partial fingerprint recognition. The previously developed fingerprint alignment methods, including minutia-based and non-minutia feature based ones, are unsuitable for partial fingerprints because small fingerprint fragments often do not have enough features required by these methods. In this paper, we propose a new approach to aligning high resolution partial fingerprints based on pores, a type of fingerprint fine ridge features that are abundant on even small fingerprint areas. Pores are first extracted from the fingerprint images by using a difference of Gaussian filtering approach. After pore detection, a novel pore–valley descriptor (PVD) is proposed to characterize pores based on their locations and orientations, as well as the ridge orientation fields and valley structures around them. A PVD-based coarse-to-fine pore matching algorithm is then developed to locate pore correspondences. Once the corresponding pores are determined, the alignment transformation between two partial fingerprints can be estimated. The proposed method is compared with representative minutia based and orientation field based methods using the established high resolution partial fingerprint dataset and two fingerprint matchers. The experimental results show that the PVD-based method can more accurately locate corresponding feature points, estimate the alignment transformations, and hence significantly improve the accuracy of high resolution partial fingerprint recognition.

1. Introduction

Automatic fingerprint recognition systems (AFRS) have been nowadays widely used in personal identification applications such as access control [1,2]. Roughly speaking, there are three types of fingerprint matching methods: minutia-based, correlation-based, and image-based [2,38]. In minutia-based approaches, minutiae (i.e. endings and bifurcations of fingerprint ridges) are extracted and matched to measure the similarity between fingerprints [13–17]. These minutia-based methods are now the most widely used ones [1,2]. Different from the minutia-based approaches, both correlation-based and image-based methods compare fingerprints in a holistic way. The correlation-based methods spatially correlate two fingerprint images to compute the similarity between them [20], while the image-based methods first generate a feature vector from each fingerprint image and then compute their similarity based on the feature vectors [24,35–38]. No matter what kind of fingerprint matchers are used, the fingerprint images usually have to be aligned when matching them. Later in this section, we will discuss more about the fingerprint alignment methods.

In order to further improve the accuracy of AFRS, people are now exploring more features in addition to minutiae on fingerprints. The recently developed high resolution fingerprint scanners make it possible to reliably extract level-3 features such as pores. Pores have been used as useful supplementary features for a long time in forensic applications [8,39]. Researchers have also studied the benefit of including pores in AFRS and validated the feasibility of pore based AFRS [3,4,7,9,10,34]. Using pores in AFRS has two advantages. First, pores are more difficult to be damaged or mimicked than minutiae [34]. Second, pores are abundant on fingerprints. Even a small fingerprint fragment could have a number of pores (refer to Fig. 1). Therefore, pores are particularly useful in high resolution partial fingerprint recognition where the number of minutiae is very limited. In this paper, we focus on the alignment of high resolution partial fingerprints and investigate the methods for high resolution fingerprint image processing.

1.1. High resolution partial fingerprint

In a live-scan AFRS, a user puts his/her finger against the prism and the contact fingerprint region will be captured in the resulting image. A small contact region between the finger and the prism will lead to a small partial fingerprint image. On such small fingerprint

---

* Corresponding author. Tel.: +852 27667271; fax: +852 27740842.
E-mail address: csdzhang@comp.polyu.edu.hk (D. Zhang).

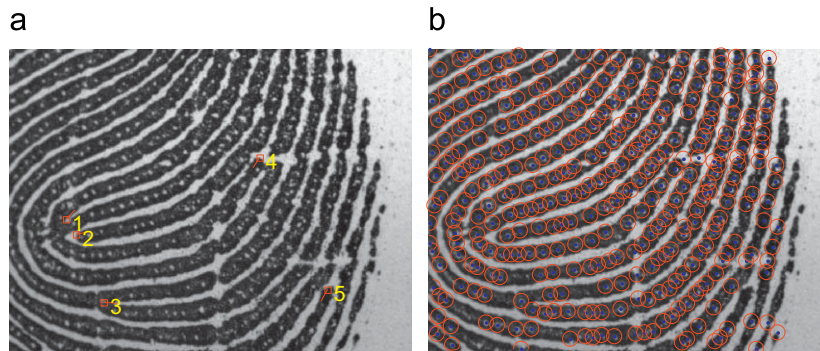a   b

Fig. 1. An example of high resolution partial fingerprint. It has only five minutiae as marked in (a), but hundreds of pores as marked in (b).

region, there could be very limited minutiae available for recognition. A natural way to solve the partial fingerprint recognition problem is to make full use of other fine fingerprint features abundant on the small fingerprint fragments. Sweat pores are such kind of features and high resolution fingerprint imaging makes it possible to reliably extract the sweat pores on fingerprints [39].

Most existing high resolution fingerprint recognition methods use full-size fingerprint images which capture large fingerprint areas. However, to capture the full fingerprints, high resolution fingerprint images should have much bigger sizes than conventional low resolution fingerprint images. As a result, much more computational resources are required to process the images. Considering the increasing demand of AFRS on mobile devices and other small portable devices, small fingerprint scanners and limited computational resources are very common [5]. Consequently, the algorithms for aligning and matching partial fingerprint images are becoming important. Therefore, this paper, different from previous study of high resolution fingerprint recognition, uses high resolution partial fingerprint images to study the partial fingerprint image alignment problem and a feasible algorithm will be proposed.

Although some methods have been proposed to construct full fingerprint templates from a number of partial fingerprint images [11], it is expensive or even impossible to collect sufficient fingerprint fragments to construct a reliable full fingerprint template. Moreover, some errors (e.g. spurious features) could be introduced in the construction process. Thus, it is meaningful and very useful if algorithms can be developed for aligning and matching partial fingerprints to partial fingerprints.

Some researchers have studied the problem of matching a partial fingerprint to full template fingerprints. In [5], Jea and Govindaraju proposed a minutia-based approach to matching incomplete or partial fingerprints with full fingerprint templates. Their approach uses brute-force matching when the input fingerprints are small and few minutiae are presented, and uses secondary feature matching otherwise. Since this approach is based on minutiae, it is very likely to produce false matches when there are very few minutiae, and it is not applicable when there are no minutiae on the fingerprint fragments. Kryszczuk et al. [3,4] proposed to utilize pore locations to match fingerprint fragments. Using high resolution fingerprint images (approx. 2000 dpi in [3,4]), they studied how pores might be used in matching partial fingerprints and showed that the smaller the fingerprint fragments, the greater the benefits of using pores. In their method, Kryszczuk et al. aligned fingerprints by searching for the transformation parameters which maximize the correlation between the input fingerprint fragment and the candidate part on the full fingerprint template. Very recently, Chen and Jain [6] employed minutiae, dots, and incipient ridges, to align and match partial fingerprints with full template fingerprints.

One drawback of most of the above approaches in aligning fragmental fingerprints is that they are mainly based on the features which are probably very few (e.g. minutiae) or even do not exist (e.g. dots and incipient ridges) on small fingerprint fragments (refer to Fig. 1). When the template fingerprints are also small fingerprint fragments, it will become difficult to get correct results due to the lack of features. In [3,4], Kryszczuk et al. proposed a correlation-based blind searching approach to fragmental fingerprint alignment. As we will show later, however, this method has limited accuracy because it has to discretize the transformation parameter space.

1.2. Fingerprint alignment

Fingerprint alignment or registration is a crucial step in fingerprint recognition. Its goal is to retrieve the transformation parameters between fingerprint images and then align them for matching. Some non-rigid deformation or distortion could occur in fingerprint image acquisition. It is very costly to model and remedy such distortions in fingerprint registration, and they can be compensated to some extent in subsequent fingerprint matching. Thus, the majority of existing fingerprint alignment methods considers only translation and rotation, although some deformable models [18,19] have been proposed. According to the features used, existing fingerprint alignment methods can be divided into two categories, minutia based and non-minutia feature based methods. Minutia based methods are now the most widely used ones [12–17,21,22,25,32,38]. Non-minutia feature based methods [20,23,24,26–29] include those using image intensity values, orientation fields, cores, etc. One problem in applying these methods to partial fingerprints is that the features required by them could be very few on the fragments. Consequently, they will either lead to incorrect results or be not applicable.

There are roughly two kinds of methods for estimating alignment transformations. The first kind of methods quantizes the transformation parameters into finite sets of discrete values and searches for the best solution in the quantized parameter space [3,4,20–22,26–29]. The alignment accuracy of these methods is thus limited due to the quantization. The second kind of methods first detects corresponding feature points (or reference points) on fingerprints and then estimates the alignment transformation based on the detected corresponding points [12–17,23–25,32]. Most of such methods make use of minutiae as the feature points. As discussed before, however, it is problematic to align partial fingerprints based on minutiae because of the lack of such features on the fingerprint fragments.

1.3. Partial fingerprint alignment based on pores

Following the second kind of alignment methods, we need to find some reference points other than minutiae on fingerprints for the purpose of aligning partial fingerprints. One possible solution is to use sufficiently densely sampled points on ridges as such reference points. However, it is hard, or even impossible, to ensure that

identical points are sampled on different fingerprint images, and a too dense sampling of points will make the matching computationally prohibitive. On the contrary, sweat pores (as well as minutiae) are unique biological characteristics and are persistent on a finger throughout the life. Compared with minutiae, they are much more abundant on small partial fingerprints. Therefore, the pores can serve as reliable reference points in aligning partial fingerprint images. Although pore shapes and sizes are also important and biophysically distinctive features [8], they cannot be reliably captured on fingerprint images because they are greatly affected by the pressure of the fingertip against the scanner. On the other hand, the pore statuses can change between open and close from time to time. Therefore, in general only the locations of pores are used in recognizing the pores and the fingerprints [39].

Considering the plenty of pores on partial fingerprints, in this paper we introduce, to the best of our knowledge, for the first time an approach to aligning partial fingerprints based on the pores reliably extracted from high resolution partial fingerprint images. This approach, by making use of the pores on fingerprints as reference feature points, can effectively align partial fingerprints and estimate the transformation between them even when there is a small overlap and large translation and rotation. We first propose an efficient method to extract pores, and then present a descriptor of pores, namely the pore–valley descriptor (PVD), to determine the correspondences between them. The PVD describes a pore using its location and orientation, the ridge orientation inconsistency in its neighborhood, and the structure of valleys surrounding it. The partial fingerprints are first matched based on their PVDs, and the obtained pore correspondences are further refined using the global geometrical relationship between the pores. The transformation parameters are then calculated from the best matched pores. The experiments demonstrate that the proposed PVD-based alignment method can effectively detect corresponding pores and then accurately estimate the transformation between partial fingerprints. It is also shown that the proposed alignment method can significantly improve the recognition accuracy of partial fingerprint recognition.

The rest of this paper is organized as follows. Section 2 presents methods for extracting pores and valleys and defines the pore–valley descriptors (PVD). Section 3 presents the PVD-based fingerprint alignment method in detail. Section 4 performs extensive experiments to verify the effectiveness of the proposed method. Section 5 concludes the paper.

2. Feature extraction

The fingerprint features, including pores, ridges and valleys, will be used in the proposed method. The extraction of ridge orientations and frequencies and ridge maps has been well studied in the literature [1,2]. In this paper, we use the classical methods proposed by Jain et al. [13,30] to extract ridge orientations, frequencies and ridge maps. Because ridges and valleys are complementary on fingerprints, it is a simple matter to get skeleton valley maps by thinning the valleys on the complement of ridge maps. To extract pores, we divide the fingerprint into blocks and use Gaussian matched filters to extract them block by block. The scales of Gaussian filters are adaptively determined according to the ridge frequencies on the blocks. After extracting orientation fields, valleys, and pores, we can then generate the pore–valley descriptor for each pore. Next we describe the feature extraction methods in detail.

2.1. Ridge and valley extraction

The considered partial fingerprint image has a higher resolution (approx. 1200 dpi in this paper) than the conventional fingerprints (about 500 dpi) so that level-3 features such as pores can be reliably

extracted from them. To extract ridges and valleys, it is not necessary to directly work on images of such a high resolution. In order to save computational cost, we smooth the image and down-sample it to half of its original resolution, and use the method in [30] to calculate the ridge orientations and frequencies. Based on local ridge orientations and frequencies, a bank of Gabor filters are used to enhance the ridges on the fingerprint. The enhanced fingerprint image is then binarized to obtain the binary ridge map.

On fingerprints, valleys and ridges are complementary to each other. Therefore, we can easily get the binary valley map as the complement of the binary ridge map. In order to exclude the effect of background on complement calculation, the fingerprint region mask [30] is employed to filter out the background if any. The binary valley map is then thinned to make all valleys be single-pixel lines. On the resulting skeleton valley map, there could be some false and broken valleys due to scars and noise. Thus we post-process it by connecting valley endings if they are very close and have opposite directions, and by removing valley segments between valley endings and/or valley bifurcations if they are very short or their orientations differ much from the local ridge orientations. Finally, we up-sample the obtained ridge orientation and frequency images, binary ridge map and skeleton valley map to the original resolution. Fig. 2(b) shows the skeleton valley map extracted from the original fingerprint fragment in Fig. 2(a).

2.2. Pore extraction

Referring to Figs. 1 and 2(a), on the fingerprint images captured using an optical contact fingerprint sensor, ridges (valleys) appear as dark (bright) lines, whereas pores are bright blobs on ridges, either isolated (i.e. closed pores) or connected with valleys (i.e. open pores). In general pores are circle-like structures and their spatial distributions are similar to 2-D Gaussian functions. Meanwhile, the cross-sections of valleys are 1-D Gaussian-like functions with different scales. To be specific, valleys usually have bigger scales than pores. Based on this observation, we use two 2-D Gaussian filters, one with a small scale and the other with a large scale, to enhance the image. The difference between their outputs can then give an initial pore extraction result. This procedure is basically the DoG (difference of Gaussian) filtering, which is a classic blob detection approach. The difficulty here is how to estimate the scales of the Gaussian filters.

Considering that the scale of either pores or valleys is usually not uniform across a fingerprint image and different fingerprints could have different ridge/valley frequencies, we partition the fingerprint into a number of blocks and estimate adaptively the scales of Gaussian filters for each block. Take a block image I_B as an example. Suppose the mean ridge period over this block is p. It is a good measure of the scale in its corresponding fingerprint block. Thus, we set the standard deviations of the two Gaussian filters to $k_1 p$ and $k_2 p$, respectively ($0 < k_1 < k_2$ are two constants). The outputs of them are

$$F_1 = G_{k_1 p} * I_B, \quad F_2 = G_{k_2 p} * I_B \tag{1}$$

$$G_\sigma(x, y) = \frac{1}{\sqrt{2\pi}\sigma} e^{-(x^2+y^2)/2\sigma^2} - m_G, \quad |x|, |y| \le 3\sigma \tag{2}$$

where '$*$' denotes convolution and m_G is used to normalize the Gaussian filter to be zero-mean. Note that the settings of k_1 and k_2 should take into consideration the ridge and valley widths and the size of pores. In our experiments, we empirically chose the values for them based on the fingerprint database we used. The filtering outputs F_1 and F_2 are further normalized to [0, 1] and binarized, resulting in B_1 and B_2. The small scale Gaussian filter $G_{k_1 p}$ will enhance both pores and valleys, whereas the large scale filter $G_{k_2 p}$ will enhance valleys only. Therefore, subtracting B_2 from B_1, we obtain the initial result of pore extraction: $P_B = B_1 - B_2$.
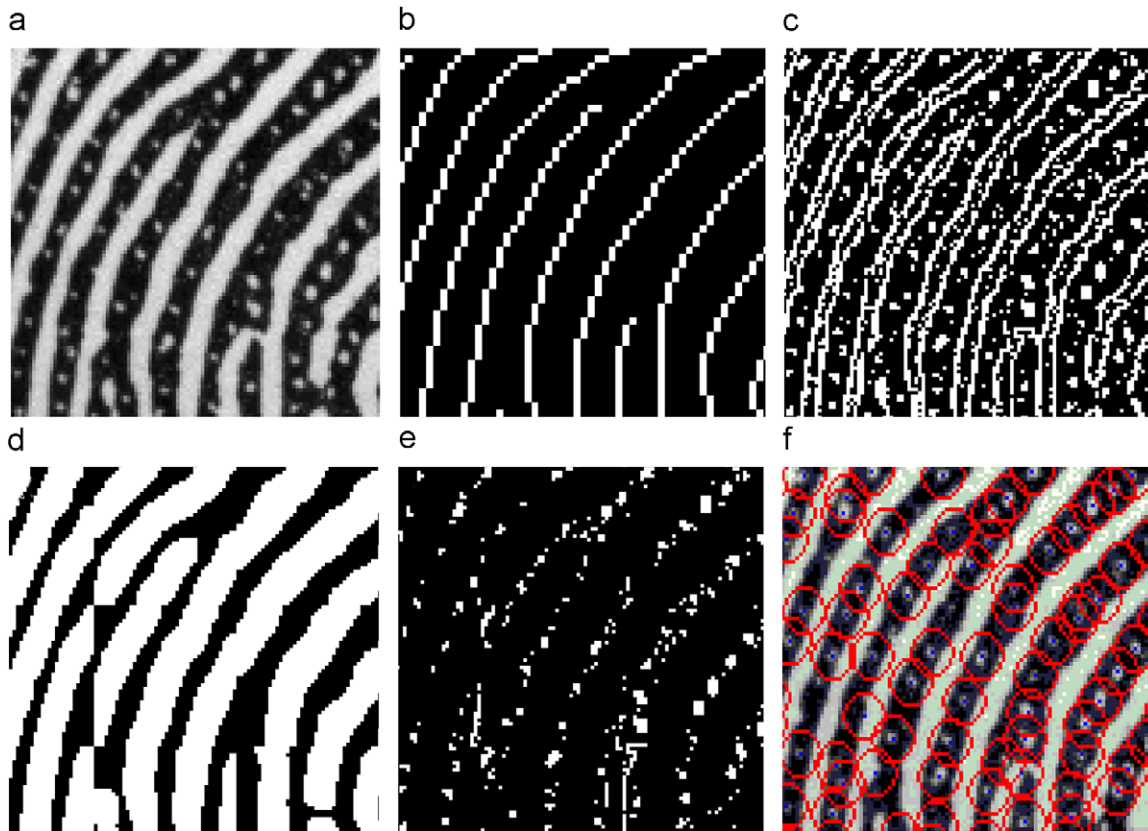
Fig. 2. (a) Original fingerprint image; (b) extracted skeleton valley map; Gaussian filtering output (c) at a small scale and (d) at a large scale; (e) difference between (c) and (d); (f) extracted pores after post-processing (pores are marked by red circles). (For interpretation of the references to color in this figure legend, the reader is referred to the web version of this article.)

To remove possible spurious pores from the initial pore extraction result P_B, we apply the following constraints to post-process the result. (1) Pores should reside on ridges only. To implement this constraint, we use the binary ridge map as a mask to filter the extracted pores. (2) Pores are circle-like features. We require that for a true pore, the eccentricity of its region should be less than a threshold. From Figs. 2(e) and (f), it can be seen that this operation can successfully remove the spurious pores caused by valley contours, i.e. those line-shaped features in Fig. 2(e). (3) Pores should be within a range of valid sizes. We measure the size of a pore by counting the pixels inside its region. In our experiments, we set the size between 3 and 30. (4) The mean intensity of a true pore region should be large enough and its variance should be small. Otherwise, the detected pores are viewed as false ones caused by noise. Finally, we get the extracted pore image. Figs. 2(c)–(f) illustrate the pore extraction process of the fingerprint in Fig. 2(a). It is worth mentioning that some other methods based on similar assumption (i.e. pores are circle-like features) have also been proposed in the literature [10,40]. Compared with those methods, the pore extraction method proposed here takes into consideration the varying pore scales and thus has better pore extraction accuracy according to our experiments. Since it is out of the scope of this paper, we do not make further discussion on this topic here due to the limit of space.

2.3. Pore–valley descriptors

In order to use pores to align fingerprints, a descriptor is needed to describe the pore features so that the correspondences between pores can be accurately determined. A good descriptor should be invariant to the deformations of rotation and translation, which are very common when capturing fingerprints. Most previous studies on pore based fingerprint recognition [3,4,9,10] describe a pore simply by its location because they compare the pores on two fingerprints with the alignment between the two fingerprints known or estimated beforehand. However, if the alignment is not given, it is not sufficient to tell one individual pore from others by using only the location feature. Thus, it is necessary to employ some other information which can be useful in distinguishing pores. According to recent work on minutia-based fingerprint recognition methods, the ridge and valley structures and the ridge orientation field surrounding minutiae are also very important in minutia matching [14,17]. Thus in this section we describe pores by using the neighboring valley structures and ridge orientation field. We call the resulting descriptor the pore–valley descriptor (PVD).

The basic attribute of a pore is its location (X, Y), which is defined as the column and row coordinates of the center of its mass. In this paper, for the purpose of alignment, we introduce the orientation feature θ for a pore. It is defined as the ridge orientation at (X, Y). Referring to Fig. 3, in order to sample the valley structures in the pore's neighborhood, we establish a local polar coordinate system by setting the pore's location as origin and the pore's orientation as the polar axis pointing to the right/bottom side. The polar angle is set as the counterclockwise angle from the polar axis. A circular neighborhood, denoted by N_p, is then chosen. It is centered at the origin with radius being $R_n = k_n p_{max}$, where p_{max} is the maximum ridge period on the fingerprint and k_n is a parameter to control the neighborhood size. Some radial lines are drawn starting from $\varphi_1 = 0°$ with a degree step θ_s until $\varphi_m = m \cdot \theta_s$, where $m = \lfloor 360°/\theta_s \rfloor$ is the total number of radial lines.
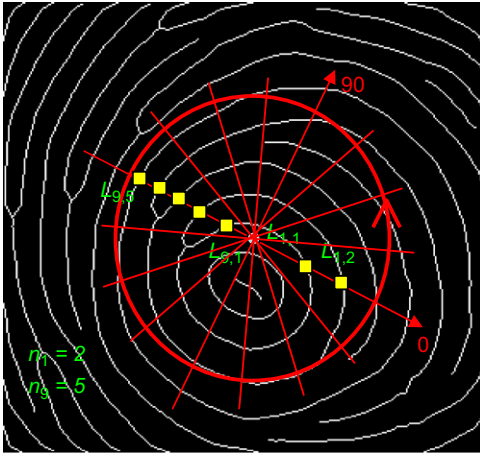
Fig. 3. Illustration of a pore–valley descriptor with $k_n = 4$ and $\theta_s = 22.5°$.

Fig. 4. Illustration of the relevant measures used in pore correspondence double checking.

For each line, we find where it intersects with valleys in the neighborhood. These intersections together with the pore give rise to a number of line segments. We number these segments from inside to outside and calculate their lengths. As shown in Fig. 3, a degree of 22.5 is taken as the step and hence 16 lines are employed. Taking the 0° and 180° lines as examples, the former has two segments and the latter has five segments. The ridge orientation field in the pore's neighborhood is another important feature. We define the ridge orientation inconsistency (OIC) in N_p as follows to exploit this information:

$$OIC(N_p) = \frac{1}{|N_p|} \sum_{(i,j) \in N_p} \{[\cos(2 \cdot OF(i,j)) - m_{\cos}]^2$$
$$+ [\sin(2 \cdot OF(i,j)) - m_{\sin}]^2\} \tag{3}$$

where OF is the ridge orientation field, $|N_p|$ denotes the number of pixels in N_p, $m_{\cos} = \sum_{(i,j) \in N_p} \cos(2 \cdot OF(i,j))/|N_p|$ and $m_{\sin} = \sum_{(i,j) \in N_p} \sin(2 \cdot OF(i,j))/|N_p|$. With the above-mentioned features, we define the PVD as the following feature vector Θ:

$$\Theta = [X, Y, \theta, OIC(N_p), \vec{S}_1, \vec{S}_2, \ldots, \vec{S}_m] \tag{4}$$

$$\vec{S}_k = [n_k, L_{k,1}, L_{k,2}, \ldots, L_{k,n_k}], \quad k = 1, 2, \ldots, m \tag{5}$$

where n_k is the number of line segments along the kth line, and $L_{k,n}$ is the length of the nth segment ($1 \le n \le n_k$) along the kth line.

The OIC component and the sampled valley structure features in the proposed PVD are invariant to rotation and translation because they are calculated in circular neighborhood of the pore which is intrinsically rotation-invariant and they are defined with respect to the local coordinate system of the pore. The OIC component is a coarse feature which captures the overall ridge flow pattern information in the neighborhood of a pore on a very coarse level. It will be used as an initial step to roughly match the pores. The sampled valley structure features are fine features. They will be used as the second step to accurately match pores. The pore locations and orientations will be used to double check pore correspondences. Finally, the transformation between fingerprints will be estimated based on the locations and orientations of their corresponding pores. In the next section, we will present the proposed PVD-based alignment algorithm.

3. PVD-based partial fingerprint alignment

This paper aims to align partial fingerprints by using pores. To this end, we need to first identify pore correspondences on fingerprints. However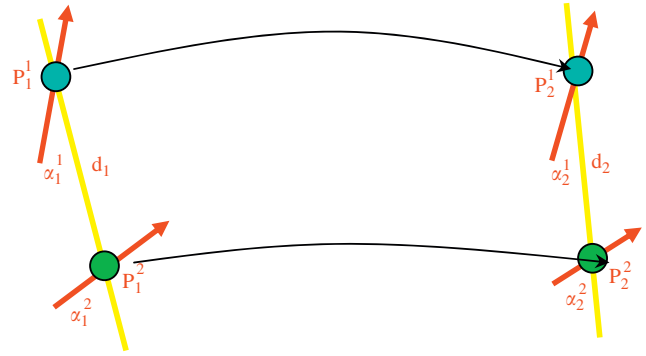, even a small fingerprint fragment can carry many pores (hundreds in the $6.24 \times 4.68\,\text{mm}^2$ fragments used in our experiments), making it very time consuming to match pores in pairs directly using their surrounding valley structures (i.e. the segment lengths recorded in the PVD). Therefore, a coarse-to-fine matching strategy is necessary. The OIC components in the PVD can serve for the coarse matching. Given two pores, we first compare their OIC features. If the absolute difference between their OIC features is larger than a given threshold T_{oic}, they will not be matched; otherwise, proceed to the next fine matching step.

Coarse matching will eliminate a large number of false matches. In the subsequent fine matching, we compare the valley structures in the two pores' neighborhoods. According to the definition of PVD, each pore is associated with several groups of line segments which capture the information of its surrounding valleys. We compare these segments group by group. When comparing the segments in the kth group, where there are n_k^1 and n_k^2 segments in the two pores' descriptors, we first find the common segments in the group, i.e. the first $\widehat{n}_k = \min\{n_k^1, n_k^2\}$ segments. The dissimilarity between the two pores is then defined as

$$\sum_{k=1}^{m} \left(\sum_{n=1}^{\widehat{n}_k} \frac{|L_{k,n}^1 - L_{k,n}^2|}{\widehat{n}_k} + \frac{(n_k^1 - n_k^2)^2}{n_k^1 \cdot n_k^2} \right) \tag{6}$$

The first term in the formula calculates the mean absolute difference between all common segments in each group, and the second term is to penalize the missing segments. The smaller the dissimilarity is, the more similar the two pores are. After comparing all possible pairs of pores which pass coarse matching, each pair of pores is assigned with a dissimilarity calculated by (6). They are then sorted ascendingly according to the dissimilarities, producing the initial correspondences between the pores.

The top K initial pore correspondences (i.e. those with the smallest degree of dissimilarity) are further double checked to get the final pairs of corresponding pores for alignment transformation estimation. The purpose of double checking is to calculate the supports for all pore correspondences based on the global geometrical relationship between the pores. At the beginning of double checking, the supports to all pore correspondences are initialized to zero. Fig. 4 illustrates the relevant measures we use.

Assume $\{P_1^1, P_2^1\}$ and $\{P_1^2, P_2^2\}$ are two pairs of corresponding pores among the top ones. To check them, we compare (1) the distances, denoted by d_1 and d_2, between the pores on the two fingerprints; and (2) the angles, denoted by $\{\alpha_1^1, \alpha_2^1\}$ and $\{\alpha_1^2, \alpha_2^2\}$, between their orientations and the lines connecting them. If both the distance differences and the angle differences are below the given thresholds T_d and T_α, i.e.

$$|d_1 - d_2| \le T_d, \quad |\alpha_1^1 - \alpha_2^1| \le T_\alpha, \quad |\alpha_1^2 - \alpha_2^2| \le T_\alpha \tag{7}$$

the supports for these two correspondences are increased by 1; otherwise, the support for the correspondence with higher dissimilarity is decreased by 1, whereas the support for the other one stays the same. After checking all the top K correspondences two by two, those with a non-negative support are taken as the final pore correspondences. If none of the correspondences has non-negative support, the two fingerprints cannot be aligned.

If some corresponding pores are found, we can then estimate the transformation between the two fingerprints. Here, we consider rotation and translation (since all the fingerprints are captured by the same type of scanner, we assume that the scaling factor is one) as follows:

$$\begin{bmatrix} \tilde{X}_2 \\ \tilde{Y}_2 \end{bmatrix} = \begin{bmatrix} \cos\beta & -\sin\beta \\ \sin\beta & \cos\beta \end{bmatrix} \begin{bmatrix} X_2 \\ Y_2 \end{bmatrix} + \begin{bmatrix} \Delta X \\ \Delta Y \end{bmatrix} = R\begin{bmatrix} X_2 \\ Y_2 \end{bmatrix} + t \quad (8)$$

where (X_2, Y_2) are the coordinates of a pore on the second fingerprint and $(\tilde{X}_2, \tilde{Y}_2)$ are its transformed coordinates in the first fingerprint's coordinate system,

$$R = \begin{bmatrix} \cos\beta & -\sin\beta \\ \sin\beta & \cos\beta \end{bmatrix}$$

is the rotation matrix and

$$t = \begin{bmatrix} \Delta X \\ \Delta Y \end{bmatrix}$$

is the translation vector. Our goal is to estimate the transformation parameters $(\beta, \Delta X, \Delta Y)$, where β is the rotation angle and ΔX and ΔY are the column and row translations, respectively.

If there is only one pair of corresponding pores found on the two fingerprints, we directly estimate the transformation parameters by the locations and orientations of the two pores, (X_1, Y_1, θ_1) and (X_2, Y_2, θ_2), as follows:

$$\beta = \begin{cases} \beta_1 & \text{if } abs(\beta_1) \le abs(\beta_2) \\ \beta_2 & \text{else} \end{cases} \quad (9)$$

$$\Delta X = X_1 - X_2 \cos\beta + Y_2 \sin\beta \quad (10)$$

$$\Delta Y = Y_1 - X_2 \sin\beta - Y_2 \cos\beta \quad (11)$$

where $\beta_1 = \theta_1 - \theta_2$ and $\beta_2 = \text{sgn}(\beta_1) \cdot (|\beta_1| - \pi)$.

If there are more than one pairs of corresponding pores, we employ the method similar to [31] to estimate the rotation and translation parameters based on the locations of the corresponding pores. Let $\{(X_1^i, Y_1^i)|i=1,2,\ldots,C\}$ and $\{(X_2^i, Y_2^i)|i=1,2,\ldots,C\}$ be C pairs of corresponding pores. We determine R and t by minimizing

$$\frac{1}{C}\sum_{i=1}^{C}\left\| \begin{bmatrix} X_1^i \\ Y_1^i \end{bmatrix} - R\begin{bmatrix} X_2^i \\ Y_2^i \end{bmatrix} - t \right\|^2 \quad (12)$$

where '$\|\cdot\|$' is the L_2-norm. Following the proof in [31], it is easy to show that

$$t = \begin{bmatrix} \bar{X}_1 \\ \bar{Y}_1 \end{bmatrix} - R\begin{bmatrix} \bar{X}_2 \\ \bar{Y}_2 \end{bmatrix} \quad (13)$$

where $\bar{X}_j = (\sum_{i=1}^{C} X_j^i)/C$, $\bar{Y}_j = (\sum_{i=1}^{C} Y_j^i)/C$, $j=1,2$. Let

$$B = \frac{1}{C}\begin{bmatrix} \sum_{i=1}^{C}(X_1^i - \bar{X}_1)(X_2^i - \bar{X}_2) & \sum_{i=1}^{C}(Y_1^i - \bar{Y}_1)(X_2^i - \bar{X}_2) \\ \sum_{i=1}^{C}(X_1^i - \bar{X}_1)(Y_2^i - \bar{Y}_2) & \sum_{i=1}^{C}(Y_1^i - \bar{Y}_1)(Y_2^i - \bar{Y}_2) \end{bmatrix} \quad (14)$$

and its singular value decomposition be $B = UDV$, then $R = VU^T$ and $\beta = \arcsin(R_{21})$, where R_{21} is the entry at the second row and first column of R.

4. Experiments

In general, the feature of pores can only be reliably extracted from fingerprints with a resolution of at least 1000 dpi [39]. So far there is no such free fingerprint image database available in the public domain. Therefore, we established a set of high resolution partial fingerprint images by using a custom-built fingerprint scanner of approximate 1200 dpi (refer to Fig. 5 for example images). With the established high resolution partial fingerprint image dataset, we evaluate the proposed fingerprint alignment method in comparison with a minutia-based method and an orientation field-based method. Next in Section 4.1 we first introduce the collected dataset of high resolution partial fingerprint images; in Section 4.2 we investigate the two parameters involved in the method; Section 4.3 compares the proposed method with the minutia based method in corresponding feature point detection; Section 4.4 compares the proposed method with the orientation field based method in alignment transformation estimation; in Section 4.5 we compare the three methods in terms of fingerprint recognition accuracy; finally, in Section 4.6 we analyze the computational complexity of the method.

4.1. The high resolution partial fingerprint image dataset

We first collected 210 partial fingerprint images from 35 fingers as the training set for parameter selection and evaluation, and then collected 1480 fingerprint fragments from 148 fingers (including the fingers in the training set) as the test set for performance evaluation[1]. The data were collected in two sessions (about two weeks apart). Most of the participants are students and staff in our institute, whose ages are between 20 and 50 years old. In the training set, there are three images captured from each finger in each session; whereas in the test set, each finger has five images scanned in each of the two sessions.

The resolution of these fingerprint images is approximately 1200 dpi and their spatial size is 320 pixels in width and 240 pixels in height. Therefore, they cover an area of about 6.5 mm by 4.9 mm on fingertips. When capturing the fingerprint images, we simply asked the participants to naturally put their fingers against the prism of the scanner without any exaggeration of fingerprint deformation. As a result, typical transformations between different impressions of the same finger in the dataset include translations with tens of pixels and rotations by around 8°. The maximal translations and rotations are, respectively, about 200 pixels and 20°. Hence, the minimal overlap between a finger's different impressions is about one fourth of the fingerprint image area. In subsequent experiments, we will give representative examples of these cases.

4.2. The neighborhood size and sampling rate of directions

The proposed alignment method uses the valley structures in the neighborhood of pores. The valley structures are sampled along a number of different directions, determined by the degree step θ_s. Here we refer to θ_s as the sampling rate of directions. Obviously, the neighborhood size and sampling rate are two critical parameters in the proposed alignment method. We set the neighborhood size as k_n times the maximum ridge period. Intuitively, a small k_n or large θ_s will cost less computational resource but will make the resulting PVDs less discriminative, whereas a large k_n or small θ_s will lead to more noise-sensitive and costly PVDs. We evaluated the effect of k_n and θ_s on the accuracy of corresponding feature point detection using 50 pairs of fingerprints which were randomly chosen from the

---

[1] Example fingerprint images are available on our website: http://www4.comp.polyu.edu.hk/~biometrics/.
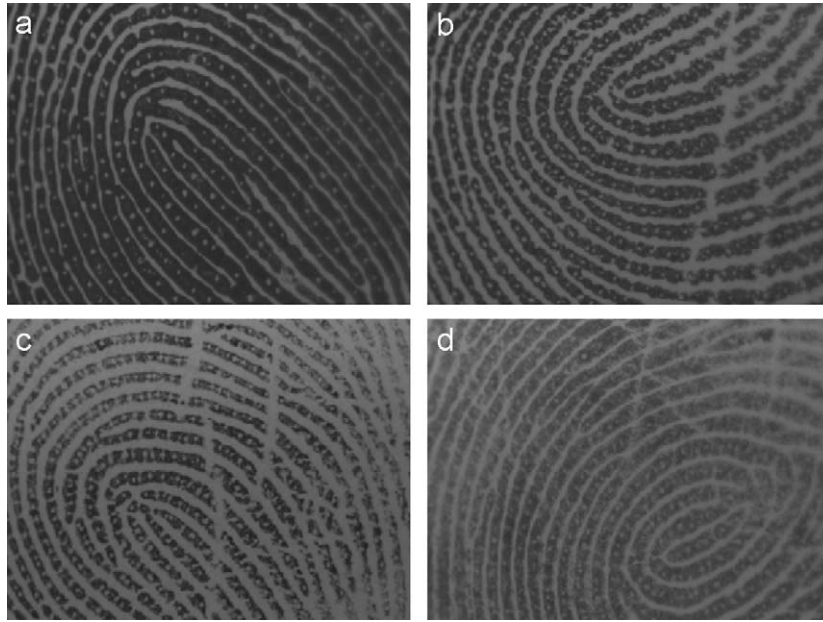
Fig. 5. Example of fingerprint images used in the experiments. Their quality indexes are (a) 0.8777, (b) 0.7543, (c) 0.6086, and (d) 0.5531 according to the frequency domain quality index defined in [33].

Table 1
Accuracies (%) of corresponding pore detection on 50 pairs of fingerprints under different settings of k_n and θ_s.

M1/M2 (%)	θ_s					
	15°	18°	20°	22.5°	30°	45°
k_n						
3	32/45.2	44/51.6	50/57.5	50/58.2	46/52.5	40/49.1
3.5	52/60.1	62/75.2	74/80.2	78/82.5	70/69.6	58/62.5
4	66/74.6	80/80.5	96/95.1	98/94.7	94/88.5	80/78.2
4.5	76/80.2	84/86	88/90.5	86/89.1	80/78.1	72/70.6
5	54/49	62/56.7	66/60.5	60/61.7	54/59.2	52/52.1

training set. Each pair is from the same finger but taken at different sessions. These fingerprints show different quality. Some example images are shown in Fig. 5.

We used two measures to evaluate the accuracy: the percentage of correct top one pore correspondence (M1) and the average percentage of correct correspondences among the top five pore correspondences (M2). Let N be the total number of pairs of fingerprint images, and N_{T1} the number of pairs of fingerprints on which the top one pore correspondence is correct. We also counted the number of correct pore correspondences among the top five correspondences on each pair of fingerprints. Denote by N_{T5}^i the number of correct pore correspondences among the top five correspondences on the ith pair of fingerprints. Then the two measures M1 and M2 are defined as

$$M1 = N_{T1}/N \tag{15}$$

$$M2 = \frac{1}{N} \sum_{i=1}^{N} N_{T5}^i / 5 \tag{16}$$

We investigated several combinations of different values for k_n and θ_s, i.e. $k_n \in \{3, 3.5, 4, 4.5, 5\}$ and $\theta_s \in \{15°, 18°, 20°, 22.5°, 30°, 45°\}$. Table 1 lists the results on the 50 pairs of fingerprints. From the results, we can see that the best accuracy is obtained at a sampling rate of $\theta_s = 20°$ or $22.5°$, and no significant difference is observed

between these two different sampling rates. With respect to the neighborhood size, it appears that $k_n = 4$ is a good choice. Furthermore, it was observed that neither too small nor too large neighborhoods can produce the best accuracy. In our following experiments, considering both the accuracy and the computational cost, we set $k_n = 4$ and $\theta_s = 22.5°$. Note that the settings of these two parameters should be dependent on the resolution of fingerprint images and the population from which the fingerprint images are captured. If a different fingerprint image dataset is used, the above training process has to be done again by using a subset of the fingerprint images in that dataset.

4.3. Corresponding feature point detection

Detecting feature point correspondences is an important step in the proposed alignment method as well as in many state-of-the-art minutia-based methods. The optimal alignment transformation is estimated based on the detected corresponding feature points (i.e. pores or minutiae). Considering the significance of corresponding feature point detection, we carried out experiments to compare the proposed method with a representative minutia-based method [32] in terms of corresponding feature point detection accuracy. In the experiments, we used 200 pairs of partial fingerprints randomly chosen from the training set for evaluation. In each pair, the two fingerprints are from the same finger but were captured at different sessions.

Fig. 6 shows some example pairs of fingerprint fragments with the detected corresponding minutiae (left column) or pores (right column). When there are more than five pairs of corresponding minutiae or pores, we show only the first five pairs. In Figs. 6(a) and (b), both methods can correctly find the top five feature point correspondences. However, when the fingerprint quality changes between sessions, for example because of perspiration, the minutiae based method will tend to detect false minutiae and hence false minutia correspondences. In Fig. 6(c), broken valleys occur on the second fingerprint. As a result, the detected two minutia correspondences are incorrect. Instead, the proposed PVD-based method is more ro-
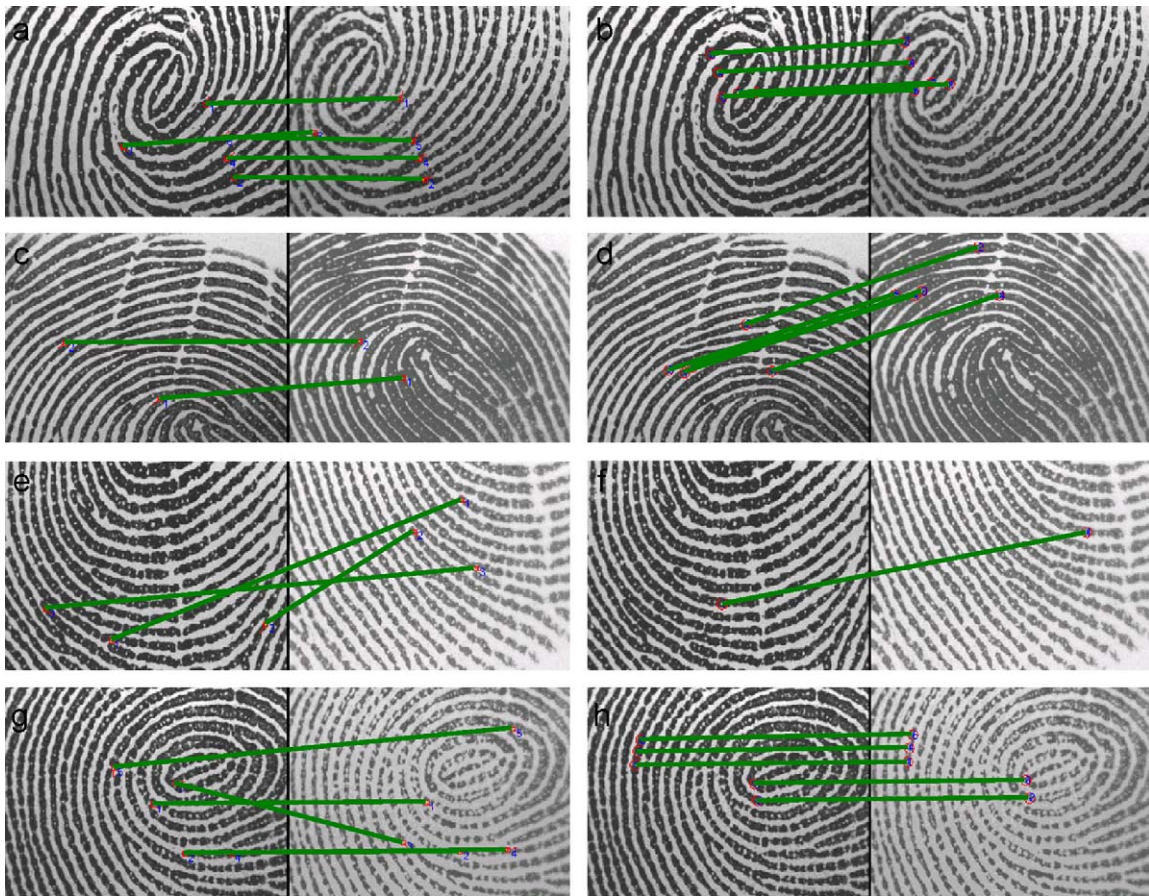
Fig. 6. Examples of corresponding feature point detection results using minutia based (left column) and PVD based (right column) methods.

Table 2
Accuracies of corresponding feature point detection by the two methods.

	M1 (%)	M2 (%)
Minutia based method [32]	40	35.1
PVD based method	98	95.5

bust and can correctly detect the corresponding pores as shown in Fig. 6(d).

The fingerprint fragments in Fig. 6(e) have large deformation and small overlap. Consequently, few (fewer than 10) minutiae can be found in their overlapping region. In this case, the minutia-based method fails again because there lack sufficient minutiae. Actually, even when two partial fingerprints overlap much, there could still be very few minutiae available on them because of the small fingerprint areas. As can be seen in Fig. 6(g), some false correspondences are detected on the two fragments due to insufficient minutiae. In contrast, as shown in Figs. 6(f) and (h), the results by the proposed PVD-based method on these partial fingerprints are much better.

We calculated the two measures, M1 and M2, for the two methods on all the 200 pairs of partial fingerprints. The results are listed in Table 2. It can be seen that the minutia-based method works poorly whereas the proposed PVD-based method can detect the corresponding feature points with a very high accuracy, achieving significant improvements over the minutia-based method. This demonstrates that the PVD-based alignment method can cope with

various fingerprint fragments more accurately than the minutia based method, largely thanks to the abundance and distinctiveness of pores on fingerprints. Since the alignment transformation estimation is based on the detected corresponding feature points, it is obvious that the PVD-based method will also estimate the alignment transformation more accurately than the minutia-based method. Next, we compare the PVD-based method with an orientation field-based method in terms of alignment transformation estimation accuracy.
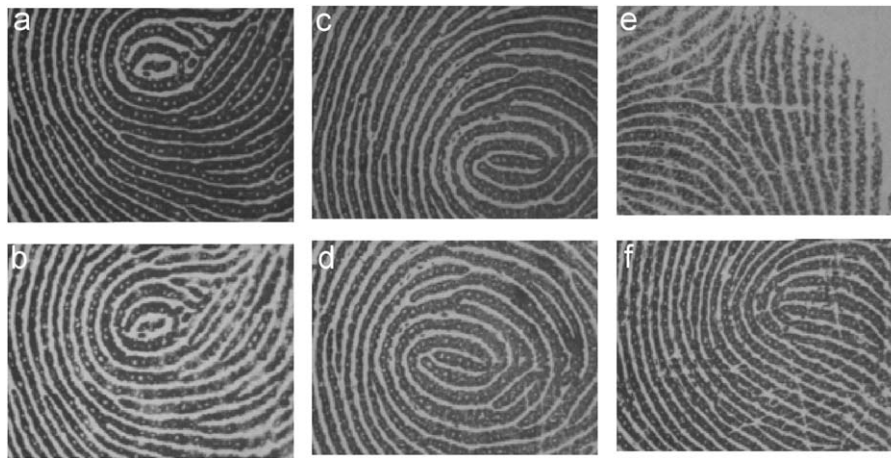
4.4. Alignment transformation estimation

After obtaining the pore correspondences on two fingerprints, we can then estimate the alignment transformation between them based on the corresponding pores. To quantitatively evaluate the performance of the proposed method in alignment transformation estimation, we need some ground truth fingerprint fragment pairs. To this end, we randomly chose 10 pairs of fingerprints from the test set (each pair was captured from the same finger but in two different sessions), and manually computed their transformations as the ground truth. Because we consider only translation and rotation here, we need at least two pairs of corresponding feature points on a pair of fingerprints to calculate the transformation between them. Therefore, we first manually marked two pairs of corresponding feature points on each of the 10 pairs of fingerprints. Based on the coordinates of the two pairs of corresponding feature points, we then directly computed the transformation between the pair of fingerprints by solving a set of equations. The obtained ground truth on

Table 3
Alignment transformation ground truth and estimation results by the two methods.

Index of fingerprint pair	Ground truth			OF based method [27]			PVD based method		
	ΔY	ΔX	β	ΔY	ΔX	β	ΔY	ΔX	β
01	−56	23	11.01	−11	3	−2.00	−61	33	13.27
02	90	33	−15.95	43	51	−1.00	93	26	−16.89
03	100	−181	−2.87	−8	72	−31.02	91	−176	2.93
04	−11	−8	−3.16	−1	1	0.00	−11	−6	−1.98
05	90	8	4.19	100	0	1.00	89	6	3.88
06	69	−74	−5.44	23	−21	0.00	72	−78	−9.33
07	78	−137	−3.45	45	−24	0.00	76	−142	−6.40
08	−87	2	0.96	−74	1	−1.00	−93	7	2.23
09	−73	39	−4.40	−69	47	−3.00	−79	50	−0.60
10	19	−4	−11.25	−4	−2	−1.00	12	−1	−8.61

Fig. 7. Three of the 10 chosen pairs of fingerprint fragments. (a, b), (c, d), and (e, f) are the first three pairs of fingerprints listed in Table 3.

the 10 pairs of fingerprints is given in Table 3. The first three pairs of fingerprints are shown in Fig. 7. From Table 3, we can see that these chosen fingerprint pairs display translations from less than 10 pixels to about 180 pixels and rotations from less than 5° to more than 10°. In our experiments, we have observed that typical transformations in the dataset are translations by tens of pixels and rotations by around 8°. In this part, we compared our proposed method with the steepest descent orientation field (OF) based alignment method [27] in terms of alignment transformation estimation accuracy using the chosen fingerprint pairs.

Table 3 lists the estimation results by the OF based method (the step sizes of translation and rotation are set as one pixel and 1°, respectively) and the proposed method on the chosen fingerprint pairs. Fig. 8 illustrates the aligned fingerprint images by overlaying the first image with the transformed second image in the pair shown in Fig. 7. Obviously, the PVD-based method estimates the transformation parameters much more accurately and it does not have the initialization and quantization problems, which will affect greatly the performance of OF based method. Moreover, there is no guarantee that the OF based method will always converge to the global optimal solution. In fact, it can be easily trapped at local minima, for example the third pair of fingerprints which has small overlap (refer to the last column in Figs. 7 and 8). In Table 4, we list the average absolute errors of the two methods over the chosen 10 fingerprint pairs. These results clearly demonstrate that the PVD-based method can recover the transformation between partial fingerprints more accurately.

4.5. Partial fingerprint recognition

We have also evaluated the proposed alignment method in partial fingerprint recognition by setting up a simple partial fingerprint recognition system as shown in Fig. 9. In this system, the alignment transformation is first estimated between an input fingerprint image and a template fingerprint image by using one of the three methods: minutia-based method, orientation field based method, and the proposed PVD based method. As for the matcher, we employed two different approaches. The first one is a minutia and pore based matcher (called MINU-PORE matcher). It matches the minutiae and pores on the fingerprints, and then fuses the match scores of minutiae and pores to give a similarity score between the fingerprints. The second approach is an image-based matcher called GLBP matcher based on Gabor and local binary patterns (LBP), recently proposed by Nanni and Lumini [38]. Note that the purpose of the experiments here is to compare the contributions of the three different alignment methods to a fingerprint matcher. Therefore, we did not do any optimization on the matchers but considered only the relative improvement between the three alignment methods.

The MINU-PORE matcher we implemented works as follows. The minutiae and pores on the input fingerprint image are transformed into the coordinate system of the template fingerprint according to the estimated transformation. Minutiae and pores on the two fingerprint images are then matched separately. Two minutiae are thought to be matched if the difference between their locations and the difference between their directions are both below the given
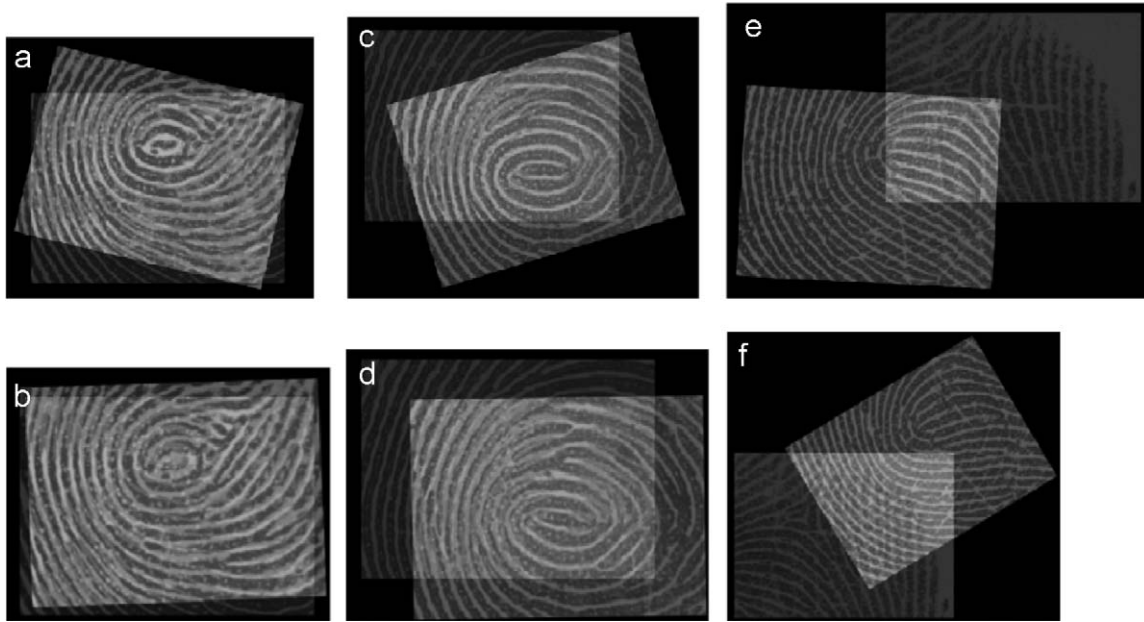
Fig. 8. Alignment results of PVD based method (a, c, e) and OF based method (b, d, f) on the fingerprint pairs shown in Figs. 7(a, b), (c, d), and (e, f).

Table 4
Average absolute errors (AAE) by the two methods.

	AAE (ΔY)	AAE (ΔX)	AAE (β)
OF based method [27]	33.9	48.5	8.5
PVD based method	4.2	5.4	2.5

Fig. 9. The simple partial fingerprint recognition system used in the experiments. FI and FT denote the input and template fingerprints, respectively.

thresholds (15 pixels for location differences and 30° for direction differences in our experiments). As for two pores, if the difference between their locations is below a given threshold (15 pixels in our experiments), they are matched. The minutia matching score is defined as the ratio between the number of matched minutiae to the total number of minutiae, and the pore matching score is defined similarly. The final matching score is obtained by fusing the minutia and pore matching scores using the summation rule.

By using the MINU-PORE matcher on the test set, we conducted the following matches. (1) Genuine matches: each of the fingerprint images in the second session was matched with all the fingerprint images of the same finger in the first session, resulting in 3700 genuine match scores. (2) Imposter matches: the first fingerprint image of each finger in the second session was matched with the first fingerprint images of all the other fingers in the first session, resulting in 21,756 imposter match scores. Based on the obtained match scores, we calculated the equal error rate (EER) of each of the three alignment methods: 29.5% by the PVD based alignment method, 38.66% by the minutia based alignment method, and 41.03% by the OF based alignment method. The receiver operating

characteristic (ROC) curves of the three methods are plotted in Fig. 10. It can be clearly seen that the proposed PVD based alignment method makes much improvement in EER, specifically 23.69% over the minutia based method and 28.1% over the OF based method.

As for the GLBP matcher, we first transform the input fingerprint image into the coordinate system of the template fingerprint image according to the estimated alignment transformation, then extract the Gabor-LBP feature vectors from the transformed input fingerprint image and the template fingerprint image (we directly took the configuration parameters from [38]), and finally calculate the Euclidean distance between the Gabor-LBP feature vectors of the input fingerprint image and the template fingerprint image. By using the GLBP matcher, we carried out the same matching scheme as in the MINU-PORE matcher. As a result, the PVD-based alignment method leads to the EER of 34.85%, the minutia based alignment method 39.98%, and the OF based alignment method 45.11%. Fig. 11 shows the corresponding ROC curves. Compared with the other two methods, the proposed PVD based alignment method achieves 12.83% and 22.74% improvement in EER, respectively. In all the experiments, it is observed that matching errors are largely caused by inaccurate alignments. This validates that the proposed alignment method is more suitable for partial fingerprints and can significantly improve the accuracy of partial fingerprint recognition. Although the EER obtained here is relatively high, this is because the recognition of partial fingerprint images is itself very challenging due to the limited features.

4.6. Computational complexity analysis

The proposed PVD based alignment method has the following main steps for each pair of fingerprint images to be aligned: (A) ridge orientation and frequency estimation; (B) ridge and valley extraction; (C) pore extraction; (D) PVD generation; (E) PVD comparison; (F) pore correspondence refinement; and (G) transformation estimation. The first two steps (A) and (B) are common to most automatic fingerprint recognition systems. The last step (G) involves a singular value decomposition of a 2×2 matrix, which can be implemented very efficiently. We have implemented the method by using Matlab and executed it on a PC with a 2.13 GHz Intel(R) Core(TM) 2 6400
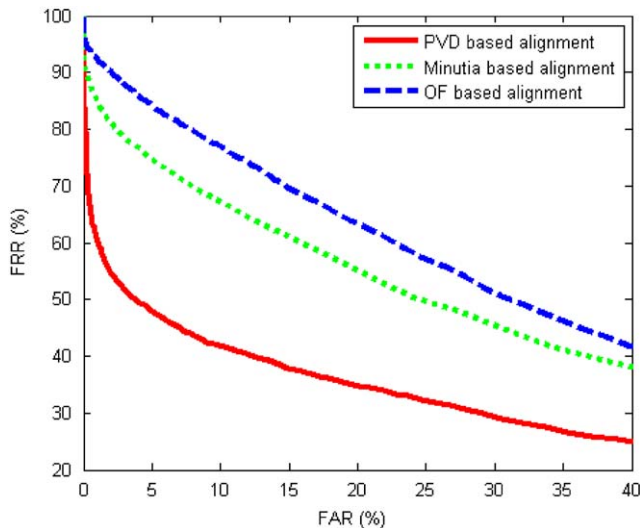
Fig. 10. The ROC curves of the MINU-PORE matcher by using the three alignment methods.
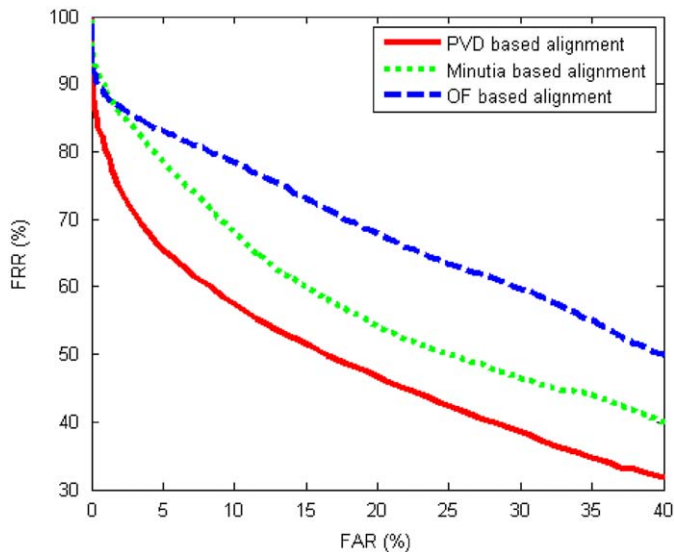

Fig. 11. The ROC curves of the GLBP matcher by using the three alignment methods.

CPU and RAM of 2 GB. It takes about 0.02 ms to estimate the transformation from a set of corresponding feature points. The step (F), pore correspondence refinement, needs to calculate some Euclidean distances and angles, which can also be done in about 0.02 ms. The step (C), pore extraction, is a little bit more time-consuming. The pore extraction method we used in this paper is a filtering based approach, which extracts pores by some linear filter operations. In our experiments, it takes about 2 s to extract the pores from a fingerprint image.

The most time-consuming steps are PVD generation (step (D)) and comparison (step (E)). Although it does not take much time to generate the PVD for one pore (about 0.02 s) or to compare the PVD of two pores (about 0.02 ms), processing the whole set of pores on fingerprints takes more time because of the large quantity of pores. With regard to the fingerprint images used in our experiments, there are averagely around 500 pores on a fingerprint fragment. Therefore, it takes in average about 10 and 5 s, respectively, to generate the PVD for the pores on a fingerprint fragment and to compare the

PVD on two fingerprint fragments. Considering that we did not optimize the code and that the Matlab code itself has low efficiency, we expect that the computational cost can be much reduced after optimization and the speed can be significantly improved by using languages like C/C++. Compared with the proposed method, the minutia based method is more efficient, taking usually less than 1 s for either extracting or matching the minutiae (but using C/C++ implementation). As for the OF based method, the time needed to align two fingerprints depends on a number of factors, such as the amount of transformation between the fingerprints, the initial estimation of the transformation, and the step sizes used in the search process. Therefore, it is difficult to draw a conclusion on its efficiency. In our experiments, the OF based method can sometimes converge in less than 1 s, but sometimes converge after more than 1 min. Generally speaking, the proposed method achieves much higher alignment accuracy than the other two approaches with an acceptable computational cost.

5. Conclusions and discussion

A new approach was proposed in this paper to aligning partial high resolution fingerprints using pores. After pore detection, a novel descriptor, namely pore–valley descriptor (PVD), was defined to describe pores based on their local characteristics. Then a coarse-to-fine pore matching method was used to find the pore correspondences based on PVD. With the detected corresponding pores, we estimated the alignment transformation between the fingerprint fragments. To evaluate the performance of the proposed PVD based high resolution partial fingerprint alignment method, we established a set of partial fingerprint images and used them to compare the proposed method with state-of-the-art minutia-based and orientation field-based fingerprint alignment methods. The experimental results demonstrated that the PVD-based method can more accurately detect the corresponding feature points and hence estimate better the alignment transformation. It was also shown in our experiments that the accuracy of partial fingerprint recognition can be significantly improved by using the PVD based alignment method.

One important issue in high resolution fingerprint recognition is the stability of pores. Despite that not all pores will appear in the fingerprint images of the same person but captured at different times, we experimentally found that usually there will be enough corresponding pores that can be detected on the fingerprint images from the same person. It is interesting and very important to further investigate the statistical characteristics of pores on fingerprint images.

Although the PVD based alignment method proposed in this paper is designed for high resolution partial fingerprint recognition, it is not limited to partial fingerprints. It can also be applied to full fingerprint images. One problem may be the expensive computational cost caused by the large amount of pore features. One solution could be to perform coarse registration first by using OF based schemes and then apply the PVD based method for a fine estimation of the alignment transformation. It also deserves to do more investigation of the discriminative power of pores.

Acknowledgments

References

[1] N. Ratha, R. Bolle, Automatic Fingerprint Recognition Systems, Springer, New York, 2004.

[2] D. Maltoni, D. Maio, A.K. Jain, S. Prabhakar, Handbook of Fingerprint Recognition, Springer, New York, 2003.

[3] K. Kryszczuk, A. Drygajlo, P. Morier, Extraction of level 2 and level 3 features for fragmentary fingerprints, in: Proceedings of the Second COST Action 275 Workshop, Vigo, Spain, 2004, pp. 83–88.

[4] K. Kryszczuk, P. Morier, A. Drygajlo, Study of the distinctiveness of level 2 and level 3 features in fragmentary fingerprint comparison, in: BioAW2004, Lecture Notes in Computer Science, vol. 3087, Springer, Berlin, 2004, pp. 124–133.

[5] T.Y. Jea, V. Govindaraju, A minutia-based partial fingerprint recognition system, Pattern Recognition 38 (2005) 1672–1684.

[6] Y. Chen, A.K. Jain, Dots and incipients: extended features for partial fingerprint matching, Presented at Biometric Symposium, BCC, Baltimore, September, 2007.

[7] A. Roddy, J. Stosz, Fingerprint features—statistical analysis and system performance estimates, Proceedings of the IEEE 85 (1997) 1390–1421.

[8] B. Bindra, O.P. Jasuja, A.K. Singla, Poroscopy: a method of personal identification revisited, Internet Journal of Forensic Medicine and Toxicology 1 (2000).

[9] J.D. Stosz, L.A. Alyea, Automated system for fingerprint authentication using pores and ridge structure, in: Proceedings of SPIE Conference on Automatic Systems for the Identification and Inspection of Humans, San Diego, vol. 2277, 1994, pp. 210–223.

[10] A.K. Jain, Y. Chen, M. Demirkus, Pores and ridges: fingerprint matching using level 3 features, IEEE Transactions on Pattern Analysis and Machine Intelligence 29 (2007) 15–27.

[11] K. Choi, H. Choi, S. Lee, J. Kim, Fingerprint image mosaicking by recursive ridge mapping, IEEE Transactions on Systems, Man, and Cybernetics—Part B 37 (2007) 1191–1203.

[12] S. Huvanandana, C. Kim, J.N. Hwang, Reliable and fast fingerprint identification for security applications, in: Proceedings of International Conference on Image Processing, vol. 2, 2000, pp. 503–506.

[13] A.K. Jain, L. Hong, R. Bolle, On-line fingerprint verification, IEEE Transactions on Pattern Analysis and Machine Intelligence 19 (1997) 302–314.

[14] M. Tico, P. Kuosmanen, Fingerprint matching using an orientation-based minutia descriptor, IEEE Transactions on Pattern Analysis and Machine Intelligence 25 (2003) 1009–1014.

[15] X. Jiang, W.Y. Yau, Fingerprint minutiae matching based on the local and global structures, in: Proceedings of International Conference on Pattern Recognition, vol. 2, 2000, pp. 1042–1045.

[16] Z.M. Kovacs-Vajna, A fingerprint verification system based on triangular matching and dynamic time warping, IEEE Transactions on Pattern Analysis and Machine Intelligence 22 (2000) 1266–1276.

[17] J. Feng, Combining minutiae descriptors for fingerprint matching, Pattern Recognition 41 (2008) 342–352.

[18] R. Cappelli, D. Maio, D. Maltoni, Modeling plastic distortion in fingerprint images, in: Proceedings of ICAPR, Rio de Janeiro, 2001.

[19] A. Ross, S. Dass, A. Jain, A deformable model for fingerprint matching, Pattern Recognition 38 (2005) 95–103.

[20] A.M. Bazen, G.T.B. Verwaaijen, S.H. Gerez, L.P.J. Veelenturf, B.J. van der Zwaag, A correlation-based fingerprint verification system, in: Proceedings of the Workshop on Circuits Systems and Signal Processing, 2000, pp. 205–213.

[21] N.K. Ratha, K. Karu, S. Chen, A.K. Jain, A real-time matching system for large fingerprint databases, IEEE Transactions on Pattern Analysis and Machine Intelligence 18 (1996) 799–813.

[22] S.H. Chang, W.H. Hsu, G.Z. Wu, Fast algorithm for point pattern matching: invariant to translations, rotations and scale changes, Pattern Recognition 30 (1997) 311–320.

[23] W. Zhang, Y. Wang, Core-based structure matching algorithm of fingerprint verification, in: Proceedings of International Conference on Pattern Recognition, vol. 1, 2002, pp. 70–74.

[24] A.K. Jain, S. Prabhakar, L. Hong, S. Pankanti, Filterbank-based fingerprint matching, IEEE Transactions on Image Processing 9 (2000) 846–859.

[25] X. Chen, J. Tian, X. Yang, Y. Zhang, An algorithm for distorted fingerprint matching based on local triangle feature set, IEEE Transactions on Information Forensics and Security 1 (2006) 169–177.

[26] N. Yager, A. Amin, Coarse fingerprint registration using orientation fields, EURASIP Journal on Applied Signal Processing 13 (2005) 2043–2053.

[27] N. Yager, A. Amin, Fingerprint alignment using a two stage optimization, Pattern Recognition 27 (2006) 317–324.

[28] L. Liu, T. Jiang, J. Yang, C. Zhu, Fingerprint registration by maximization of mutual information, IEEE Transactions on Image Processing 15 (2006) 1100–1110.

[29] A. Ross, J. Reisman, A.K. Jain, Fingerprint matching using feature space correlation, in: Proceedings of Post-European Conference on Computer Vision Workshop on Biometric Authentication, Lecture Notes in Computer Science, vol. 2359, Springer, Berlin, 2002, pp. 48–57.

[30] L. Hong, Y. Wan, A.K. Jain, Fingerprint image enhancement: algorithms and performance evaluation, IEEE Transactions on Pattern Analysis and Machine Intelligence 20 (8) (1998) 777–789.

[31] R.M. Haralick, H. Joo, C. Lee, X. Zhuang, V.G. Vaidya, M.B. Kim, Pose estimation from corresponding point data, IEEE Transactions on Systems, Man, and Cybernetics 19 (1989) 1426–1446.

[32] X. Chen, J. Tian, X. Yang, A new algorithm for distorted fingerprints matching based on normalized fuzzy similarity measure, IEEE Transactions on Image Processing 15 (2006) 767–776.

[33] Y. Chen, S. Dass, A. Jain, Fingerprint quality indices for predicting authentication performance, in: Proceedings of AVBPA, 2005, pp. 160–170.

[34] S.T.V. Parthasaradhi, R. Derakhshani, L.A. Hornak, S.A.C. Schuckers, Time-series detection of perspiration as a liveness test in fingerprint devices, IEEE Transactions on Systems, Man, and Cybernetics—Part C 35 (2005) 335–343.

[35] A. Ross, A. Jain, J. Reisman, A hybrid fingerprint matcher, Pattern Recognition 36 (2003) 1661–1673.

[36] A. Teoh, D. Ngo, O.T. Song, An efficient fingerprint verification system using integrated wavelet and Fourier–Mellin invariant transform, Image and Vision Computing 22 (6) (2004) 503–513.

[37] L. Nanni, A. Lumini, A hybrid wavelet-based fingerprint matcher, Pattern Recognition 40 (11) (2007) 3146–3151.

[38] L. Nanni, A. Lumini, Local binary patterns for a hybrid fingerprint matcher, Pattern Recognition 41 (11) (2008) 3461–3466.

[39] CDEFFS, Data format for the interchange of extended fingerprint and palmprint features, Working Draft Version 0.2 ⟨http://fingerprint.nist.gov/standard/cdeffs/index.html⟩, January 2008.

[40] M. Ray, P. Meenen, R. Adhami, A novel approach to fingerprint pore extraction, in: Proceedings of the 37th South-eastern Symposium on System Theory, 2005, pp. 282–286.

About the Author—QIJUN ZHAO holds a B.S. degree in computer science and technology from the Department of Computer Science and Engineering, Shanghai Jiao Tong University, Shanghai, P.R. China. He received his M.S. degree in computer software and theory there in 2006. He is now a Ph.D. candidate at the Department of Computing of the Hong Kong Polytechnic University and a member of the Biometrics Research Center there. His research interests include fingerprint recognition, facial expression analysis, information security, machine learning, statistical pattern recognition, computational intelligence and computational aesthetics.

About the Author—DAVID ZHANG graduated in Computer Science from Peking University. He received his M.Sc. in Computer Science in 1982 and his Ph.D. in 1985 from the Harbin Institute of Technology (HIT). From 1986 to 1988 he was a Postdoctoral Fellow at Tsinghua University and then an Associate Professor at the Academia Sinica, Beijing. In 1994 he received his second Ph.D. in Electrical and Computer Engineering from the University of Waterloo, Ontario, Canada. Currently, he is a Head, Department of Computing, and a Chair Professor at the Hong Kong Polytechnic University where he is the Founding Director of the Biometrics Technology Centre (UGC/CRC) supported by the Hong Kong SAR Government in 1998. He also serves as Visiting Chair Professor in Tsinghua University, and Adjunct Professor in Peking University, Shanghai Jiao Tong University, HIT, and the University of Waterloo. He is the Founder and Editor-in-Chief, International Journal of Image and Graphics (IJIG); Book Editor, Springer International Series on Biometrics (KISB); Organizer, the International Conference on Biometrics Authentication (ICBA); Associate Editor of more than 10 international journals including IEEE Transactions and Pattern Recognition; Technical Committee Chair of IEEE CIS and the author of more than 10 books and 200 journal papers. Professor Zhang is a Croucher Senior Research Fellow, Distinguished Speaker of the IEEE Computer Society, and a Fellow of both IEEE and IAPR.

About the Author—LEI ZHANG received the B.S. degree in 1995 from Shenyang Institute of Aeronautical Engineering, Shenyang, P.R. China, the M.S. and Ph.D degrees in Electrical and Engineering from Northwestern Polytechnical University, Xi'an, P.R. China, respectively, in 1998 and 2001. From 2001 to 2002, he was a research associate in the Department of Computing, The Hong Kong Polytechnic University. From January 2003 to January 2006 he worked as a Postdoctoral Fellow in the Department of Electrical and Computer Engineering, McMaster University, Canada. Since January 2006, he has been an Assistant Professor in the Department of Computing, The Hong Kong Polytechnic University. His research interests include Image and Video Processing, Biometrics, Pattern Recognition, Computer Vision, Multisensor Data Fusion and Optimal Estimation Theory, etc.

About the Author—NAN LUO received the B.S. degree in 2003 and he is now working as a Research Assistant at the Biometrics Research Centre of the Hong Kong Polytechnic University. His research interests include imaging technology and biometric systems.